Supporting Information

Solution-mediated Nanometric Growth of α-Fe₂O₃ with Electrocatalytic Activity for Water Oxidation

Asako Taniguchi[a,b*], Yuta Kubota[c], Nobuhiro Matsushita[c], Kento Ishii[b], Tetsuo Uchikoshi[b]

[a]Graduate School of Pure and Applied Sciences, University of Tsukuba, 1-1-1 Tennodai, Tsukuba, Ibaraki 305-8573, Japan

[b]Research Center for Functional Materials, National Institute for Materials Science (NIMS), 1-2-1 Sengen, Tsukuba, Ibaraki 305-0047, Japan

[c]Department of Materials Science and Engineering, School of Materials and Chemical Technology, Tokyo Institute of Technology, 2-12-1 Ookayama, Meguro-ku, Tokyo 152-8550, Japan
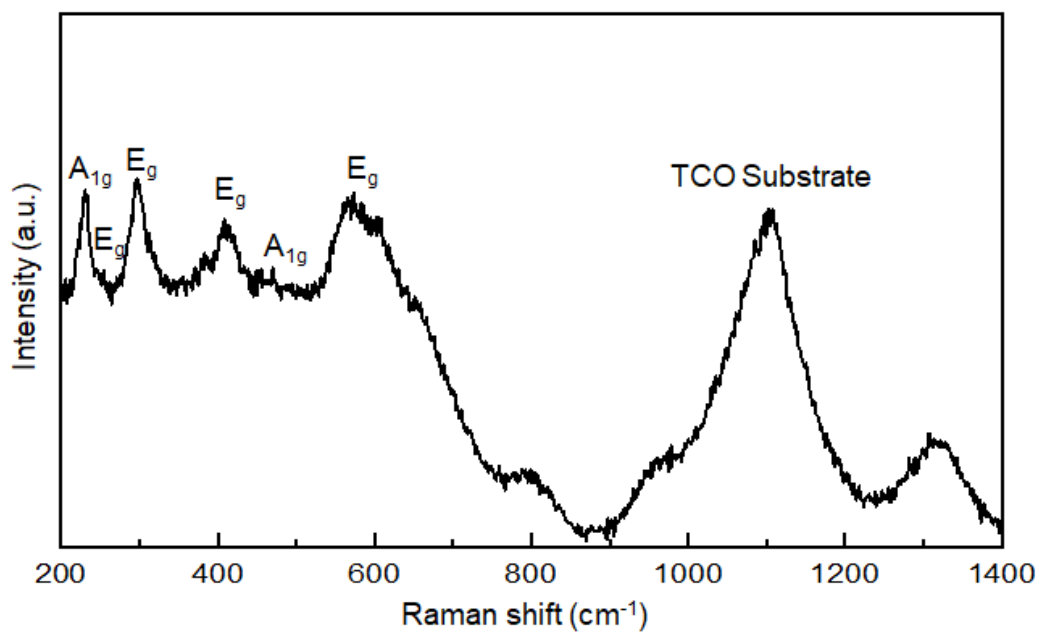
Figure S1. Wide-range Raman spectrum of SMART-derived α-Fe$_2$O$_3$ on a glass substrate deposited after 90 cycles.
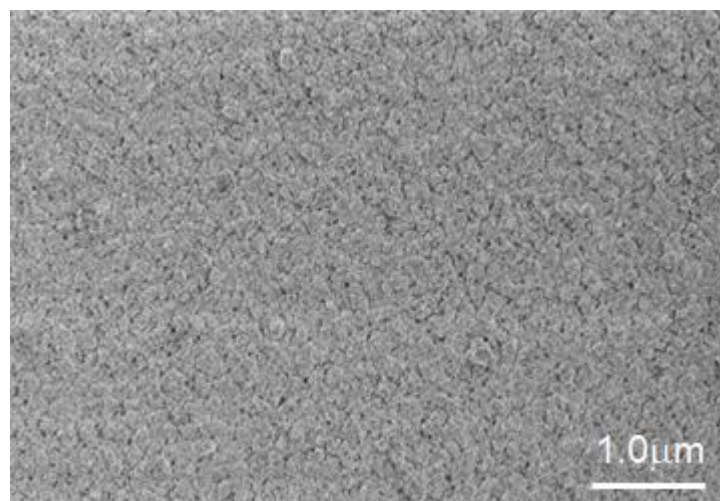
Figure S2. Low magnification SEM image of SMART-derived α-Fe$_2$O$_3$ layer on a glass substrate after 90 deposition cycles.
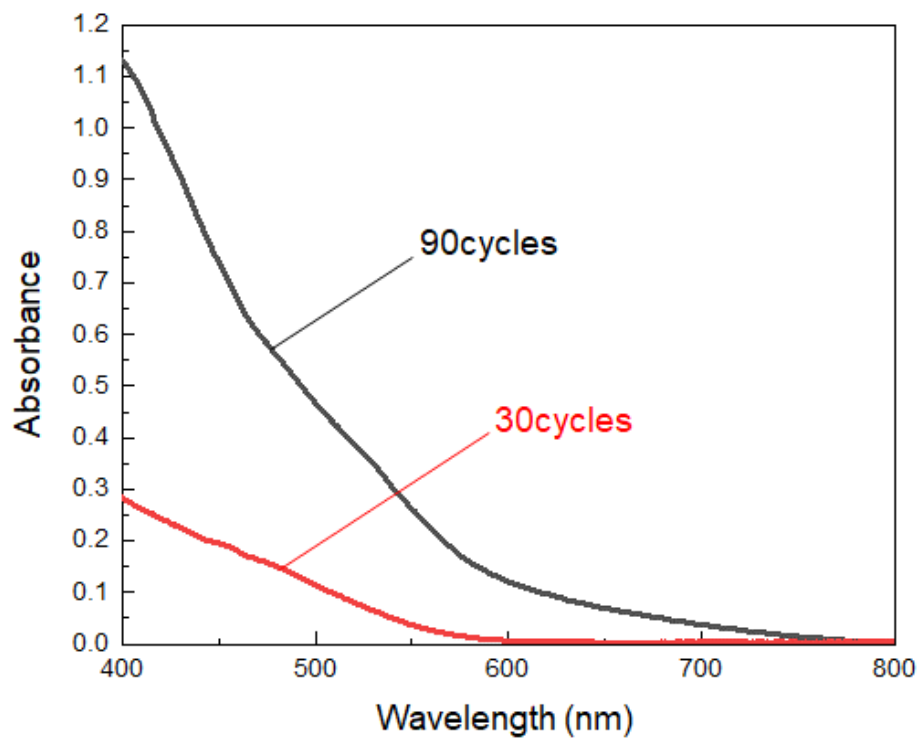
Figure S3. UV-vis spectra of SMART-derived α-Fe$_2$O$_3$ layer on a glass substrate after 30 and 90 deposition cycles.
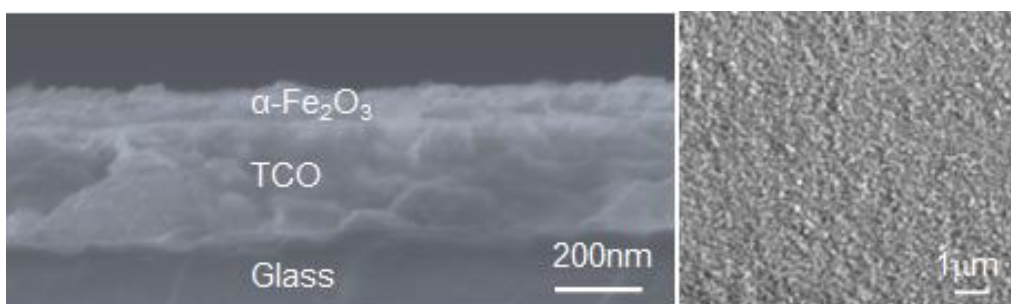
Figure S4. SEM images of SMART-derived α-Fe$_2$O$_3$ on an TCO substrate deposited after 30 cycles.
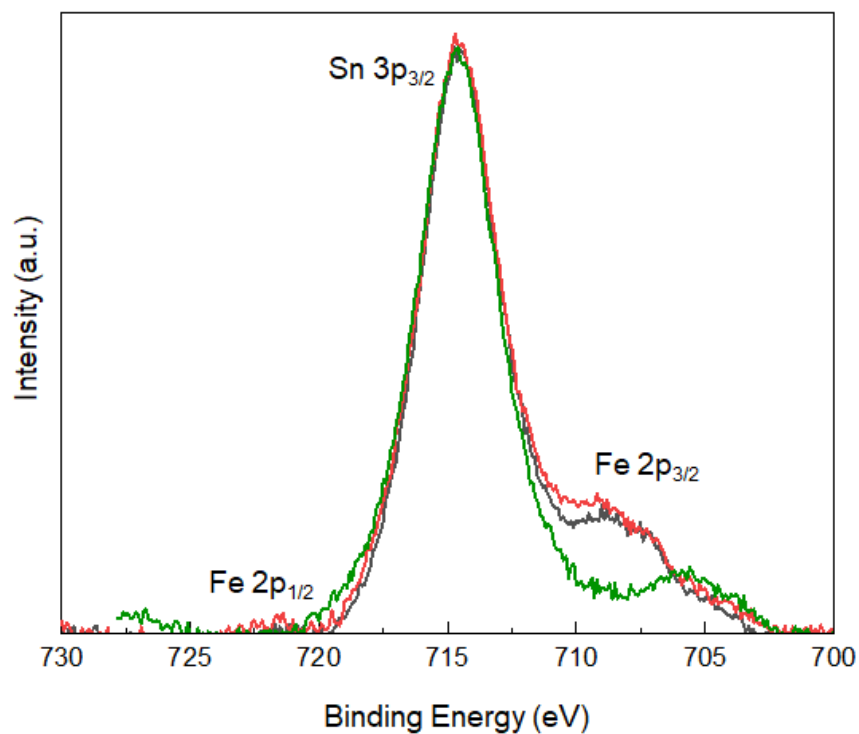
Figure S5. As-measured Fe 2p XPS spectra after the first step (black) and second step (red) in the first deposition cycle, and Sn 3p spectra of a bare TCO substrate (green).
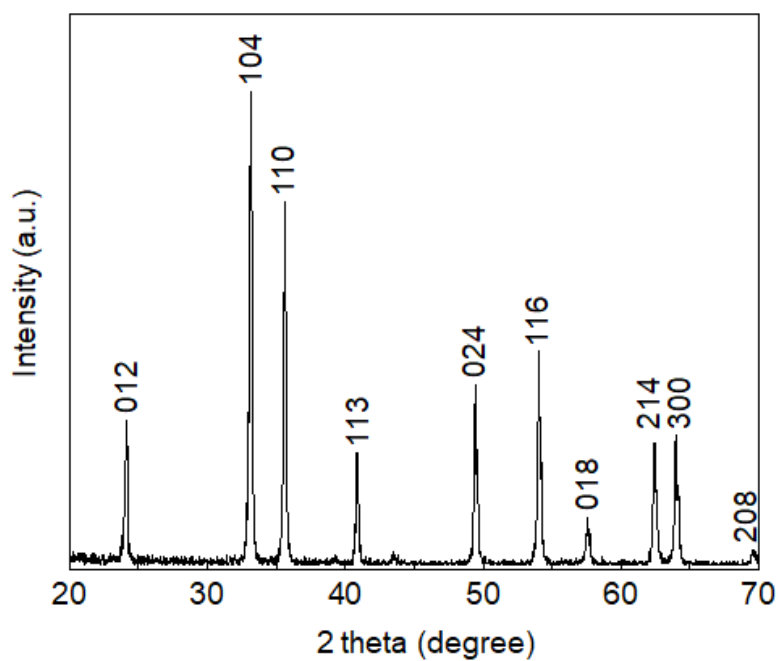
Figure S6. XRD pattern of reference α-Fe$_2$O$_3$ powder.
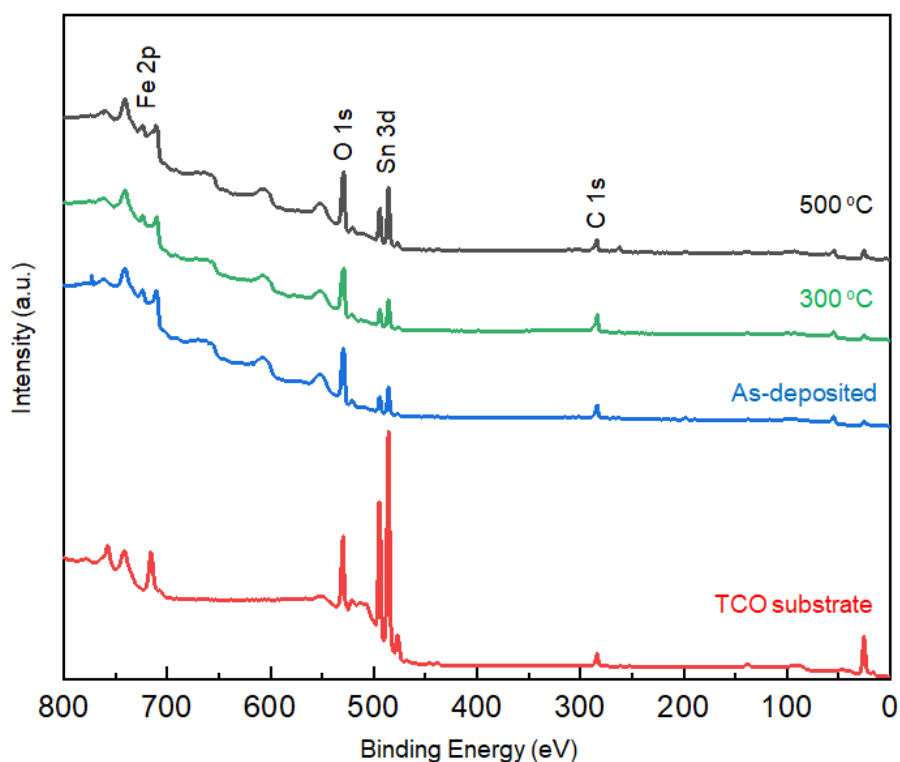
Figure S7. Wide-scan XPS spectrum of the SMART-derived α-Fe_2O_3 deposited on an TCO substrate, as-deposited, and subsequently annealed at 300 °C and 500 °C. Wide-scan XPS spectrum of TCO substrate is shown as a reference.
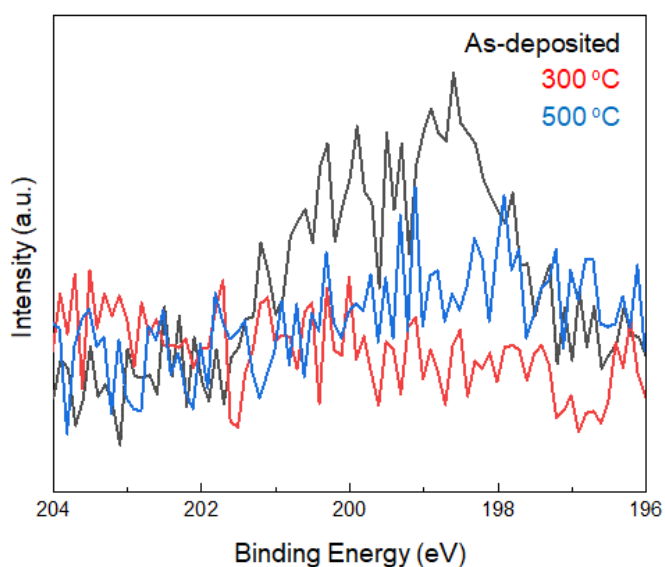
Figure S8. Cl 2p spectra of the SMART-derived α-Fe_2O_3 deposited on an TCO substrate, as-deposited, and after annealing at 300 °C and 500 °C.

(a)

[MAP 1]

Fe Kα   Ni Lα

5.0μm   10μm   10μm

Element	Wt %	At %	σ	Net Int.	K-Ratio	Line
Fe	15.90	28.66	0.18	28265	0.0202418	K
Ni	0.02	0.03	0.08	112	0.0000078	L
Sn	84.08	71.31	0.24	653167	0.0804101	L
Total	100.00	100.00				

(b)

[MAP 2]

Fe Kα   Ni Lα

5.0μm   10μm   10μm

Element	Wt %	At %	σ	Net Int.	K-Ratio	Line
Fe	14.91	26.91	0.18	28951	0.0188464	K
Ni	0.98	1.69	0.08	6614	0.0004165	L
Sn	84.10	71.40	0.23	712416	0.0797225	L
Total	100.00	100.00				
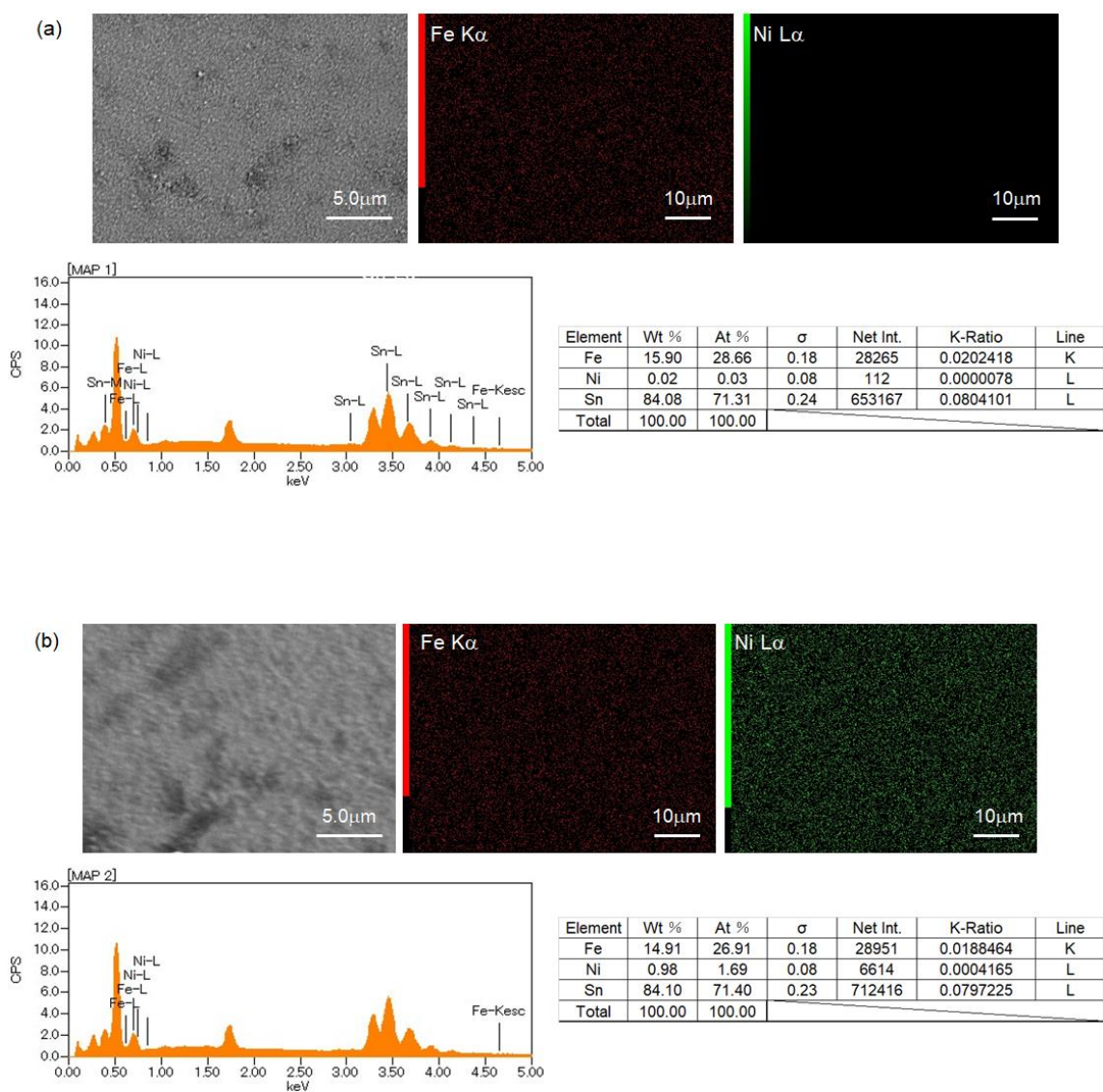
Figure S9. SEM images and Fe/Ni distributions obtained by EDS elemental mapping of SMART-derived α-Fe$_2$O$_3$ (a) before and (b) after Ni(OH)$_2$ surface-modification.
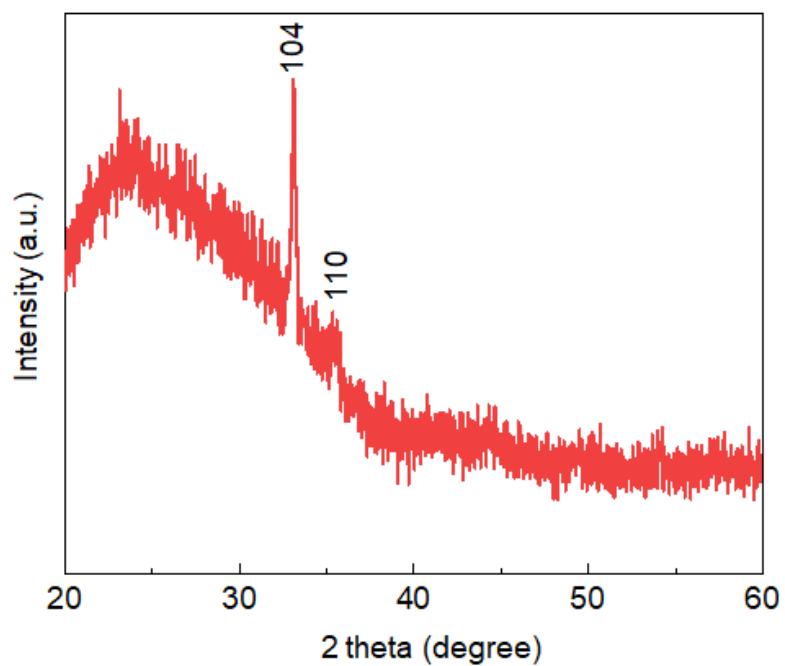
Figure S10. XRD pattern of the SMART-derived α-Fe$_2$O$_3$ (annealed at 500 °C) after Ni(OH)$_2$ surface-modification. Note that α-Fe$_2$O$_3$ layer was deposited after 90 cycles.
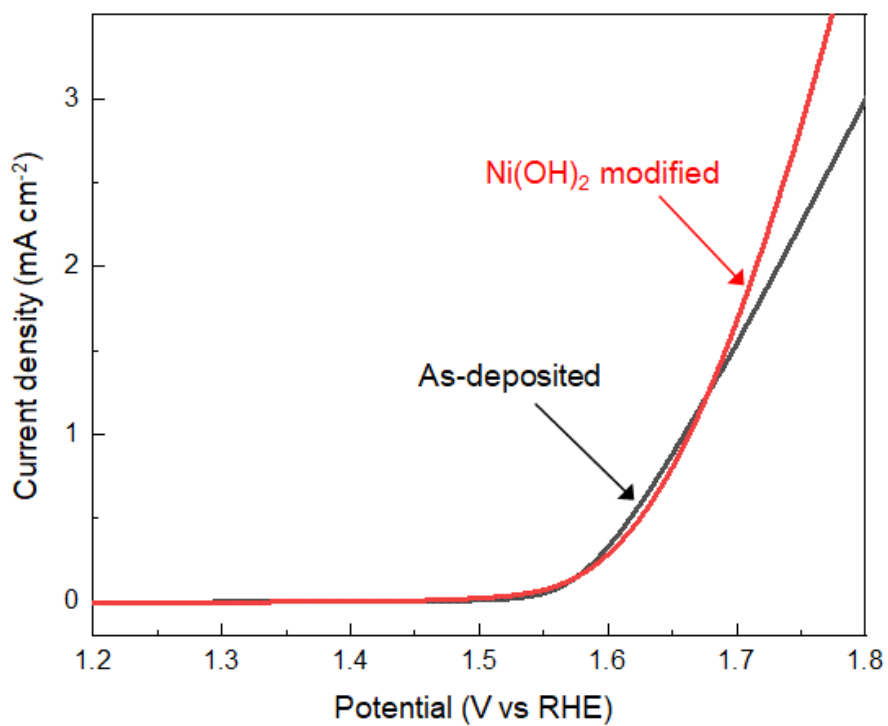
Figure S11. LSV-curves of the SMART-derived α-Fe$_2$O$_3$ before/after Ni(OH)$_2$ surface-modification.